Research Square

Preprints are preliminary reports that have not undergone peer review.
They should not be considered conclusive, used to inform clinical practice,
or referenced by the media as validated information.

Spatiotemporal Distribution Characteristics and Variations of Fog in Shandong Province, China from 2008-2019

Weixi Shu (shuweixi19@mails.ucas.ac.cn)
Institute of Atmospheric Physics Chinese Academy of Sciences
Hui Xiao
Danhong Fu
Bingsong Chang
Qiang Feng
Shujing Shen
Huiling Yang

Research Article

Keywords: Fog, Spatial-temporal distribution, Variation, Impact factors, Seasonal cycle

Posted Date: April 11th, 2022

DOI: https://doi.org/10.21203/rs.3.rs-1407603/v1

License: This work is licensed under a Creative Commons Attribution 4.0 International License.
Read Full License

Abstract

Fog has a significant effect on people's daily productivity and livelihood. The spatiotemporal distribution characteristics and variations of fog days and their impact factors in Shandong Province, China were explored by using diverse meteorological data. The results showed that the spatial distribution of fog days in Shandong province was consistent with the topographic characteristics. A few fog days region appeared a northeast-southwest trending zone in the central region, where was higher altitude topography, and more fog days on both sides can be found at lower altitude areas. Due to the effect of the topography, the water vapor transport and convergence played important roles in the spatial distribution of fog days. The annual number of fog days of different levels (light fog, dense fog, and extreme fog) in Shandong Province from 2008 to 2019 showed an increasing trend. The increase in water vapor, aggravation in air pollution, and decrease in wind speed had important effects on the increase of fog frequency. The fog frequencies in different months and seasons varied obviously, which related to the variations in LTS (lower-tropospheric stability) and wind speed in the lower layer. Fog occurred frequently within 00:00–08:00 during 2016–2019 in Shandong Province, and the diurnal variation in temperature was responsible for the diurnal variation in fog frequency. This research can serve as helpful references for the location and operation time of the work of artificial dissipating fog, and for traffic and airport safety management and control in Shandong Province.

1. Introduction

Fog, a highly complex atmospheric phenomenon, is formed when the air temperature drops to or below the dew point (i.e., in either a saturated or a supersaturated state) or near the dew point when there are a sufficient number of effective condensation nuclei (WMO 1992; Roach 1994; Kim et al. 2020). This common weather phenomenon has important impacts on people's daily productivity and livelihood (Bartok et al. 2012). For example, due to the reduced visibility in foggy weather, persistent heavy fog can paralyze road traffic, delay flights, and even cause fatal road and air traffic accidents (Bartok et al. 2012). Additionally, because of the temperature inversion that occurs on fog days, fog can induce serious harm to human health if many pollutants are present (Fu et al. 2014). Furthermore, fog can shorten the sunshine duration, which can impact crop yields (Niu et al. 2010a). Other studies have shown that fog has significant impacts on the environment, regional climate, atmospheric radiation budget, air quality, animals and plants, etc. (Shi et al. 2008; Bartok et al. 2012; Safai et al. 2019).

Given the abovementioned facts, research on the spatial and temporal distribution characteristics and their influencing factors is of great significance. Accordingly, these topics have consistently been the key subject of fog research in various regions throughout China and other countries, and many methods have been developed to investigate the statistical characteristics of fog and its impact factors in the study area (Peace 1969; Jenamani 2012; Tao et al. 2012). For instance, many researchers have employed long-term meteorological data in different places to analyze the horizontal distribution, interdecadal variation, and annual variation in fog (Zhang et al. 2009; Niu et al. 2010b; Hunova et al. 2019). Some researchers have also used atmospheric circulation data to analyze and summarize the meteorological factors and

weather patterns affecting the climatic characteristics of fog (Meyer and Lala 1990; Fu et al. 2014). Over the past few decades, the occurrence frequency of fog has decreased in some areas, and this trend is related to changes in the environment, global climate, and other factors (Lange et al. 2003; Witiw and Ladochy 2008; Vautard et al. 2009; Ye 2009; Ladochy and Witiw 2011). Liu et al. (2005) believed that the rise of minimum temperature in winter is not conducive to the formation of fog. Ding and Liu (2014) considered that the decrease in fog days in China is related to the decrease in surface relative humidity (RH) after 1990. van Oldenborgh et al. (2010) found that the changes in large-scale circulation are correlated with the decline of fog days over most of Europe in the past three decades. However, only a few studies reported that the occurrence frequency of fog has increased and signified that this change is related to the aggravation of environmental air pollution (Syed et al. 2012; Shrestha et al. 2018).

Shandong Province is located in the eastern area of China and is bounded by the Yellow Sea, the Bohai Sea, and the Taihang Mountains. It boasts the second-largest population among all provinces in China and is characterized by rapid economic development, which leads to urbanization and the aggravation of air pollution in Shandong Province. With air pollution, the frequency of heavy fog has seriously affected the productivity and livelihood of people in Shandong Province. For instance, a heavy fog event on February 11, 2009, caused 21 consecutive major traffic accidents on the Cangshan section of Beijing-Shanghai Expressway, resulting in 47 vehicle collisions and 5 deaths (http://news.cctv.com/china/20090212/106786.shtml). Wang et al. (2014) analyzed four heavy fog events in Jinan from March 2012 to February 2014 and classified the events into three types: radiation fog, advection fog, and frontal fog; they found that when fog occurred, the average surface temperature was between 0°C and 10°C, and the RH was approximately 90%. Ma et al. (2015) studied fog in Qingdao and found that the average annual number of fog days was 55 and fog weather was often accompanied by varying degrees of air pollution. Fu et al. (2006) simulated a case of heavy fog around the Shandong Peninsula and found that advection cooling plays an important role in the formation of fog.

These previous studies on fog in Shandong Province focused mainly on individual cases or a single city. However, the spatiotemporal distribution characteristics and variations (including the interannual, seasonal, and diurnal variations) of fog and its impact factors such as meteorological conditions, terrain altitude, and air pollution in Shandong Province has failed to be comprehensively studied.

For these reasons, this paper statistically analyzed meteorological observation data from 123 surface meteorological stations in Shandong Province from 2008 to 2019 to obtain the overall spatiotemporal distribution characteristics and variations (including interannual, seasonal, and diurnal variations) in fog throughout this region. For spatial distribution, the quantitative relative effects of altitude, daily average RH, and DTR on the spatial distribution of fog days were obtained. Then, this paper analyzed the characteristics of meteorological elements on both fog and non-fog days under the terrain conditions. For temporal distribution and variations, this paper discussed the possible influencing factors of annual, seasonal, and diurnal variations of fog frequency in recent years. Therefore, the mechanisms responsible for its spatiotemporal distribution characteristics and variations were obtained. The results of this study can be used as a basis for further research of fog in Shandong Province. In addition, this research can

serve as helpful references for the location and operation time of the work of artificial dissipating fog, and for traffic and airport safety management and control in Shandong Province.

2. Data And Methods

2.1. Research area and dataset

The surface meteorological stations data used in this study were obtained from 123 conventional ground meteorological stations of the ground observation network of China National Meteorological Data Center (http://data.cma.cn/en/) deployed in 17 prefecture-level cities (Jinan, Qingdao, Yantai, Weifang, etc.) within Shandong Province (Fig. 1). This dataset includes daily and hourly observation data from 2008–2019, including weather phenomena, visibility (VIS), RH, air temperature (TEM), and horizontal wind speed (among them, the complete hourly visibility data only include 2016–2019). The original data of the dataset were strictly controlled and checked, and the data passed the climatology limit value check, climate extreme value check, and internal consistency and temporal consistency checks. Moreover, missing data and abnormal data were filled with the default values (http://data.cma.cn/en/). Ground meteorological station data of China has been used in many meteorological studies (Fu et al. 2018; Chen et al. 2019).

This study utilized the fifth-generation European Centre for Medium-Range Weather Forecasts (ECMWF) Reanalysis (ERA5) product (https://www.ecmwf.int/) to analyze impact factors of the spatiotemporal distribution characteristics and variations of fog in Shandong Province during the 2008–2019 period. This data had a horizontal resolution of 0.25° × 0.25°.

2.2. Methodology

Both severe haze and other weather phenomena (such as rain, snow, sand, and dust storms) can also contribute to low visibility over China (Ding and Liu 2014). Therefore, it is necessary to differentiate between fog and other low-visibility events when analyzing trends, distributions, and variations in fog. In this work, a day was defined as a fog day when RH ≥ 90% and VIS ≤ 1 km or a haze day when RH ≤ 80% and VIS ≤ 10 km (Schichtel et al. 2001; Doyle and Dorling 2002; Qiu and Chen 2005; Ding and Liu 2014) in Shandong Province. Other low-visibility weather phenomena, such as rain, snow, sand, and dust storms, were excluded. On this basis, the fog was divided into three levels: the visibility of light fog is 0.5-1.0 km, that of dense fog is 0.2–0.5 km, and that of extreme fog is less than 0.2 km. This classification demonstrated that fog becomes heavier with decreasing visibility. Many researchers have found that aerosol pollution can be indicated by haze days (Quan et al. 2011; Yang et al. 2016). Therefore, we use haze days as the proxy for air pollution due to the absence of long-term aerosol site observational data in this paper.

The annual and seasonal variation trends of the three levels of fog during 2008–2019 were characterized by a 3-year moving average of the annual and seasonal numbers of fog days. The Cressman interpolation method, which was first proposed by Cressman (1959) of the National Weather Service

(NWS) and has been widely used in the interpolation of meteorological data, was adopted for spatial interpolation. According to this method, the weight coefficient of each neighboring data point is determined according to the distance between each neighboring data point and the interpolation point (Li et al. 2019). The meteorological station data were interpolated to longitude and latitude grid points with a spatial resolution of 0.1°×0.1°, which can more clearly reflect the spatial distribution characteristics of fog.

3. Results And Discussion

According to statistics, in the 12 years from 2008 to 2019, the spatially average number of total fog days in Shandong Province was 218 (the spatially annual average was 18 days). The number of total fog days observed at most stations concentrated between 90 and 270 days. Eighty-five percent of the stations reported fewer than 300 fog days (Fig. 2a). However, some special stations observed more than 600 fog days: Taishan station at a high altitude of 1533.7 m reported 1054 days, and Chengshantou station reported 693 days. The spatially averaged number of light fog days was 74 (the spatially annual average was 6 days), accounting for 33.9% of the total fog days. Most stations reported between 35 and 110 light fog days, while a few stations experienced more than 600 fog days (Fig. 2b). The spatially averaged number of dense fog days was 53 (the spatially annual average was 4 days). The number of dense fog days observed at most stations concentrated between 25 and 70, and nearly 100% of all stations reported fewer than 150 dense fog days (Fig. 2c). The spatially averaged number of extreme fog days was 90 (the spatially annual average was 8 days). Most stations reported between 25 and 160 extreme fog days (Fig. 2d). Compared with light fog and dense fog days, extreme fog days were more widely distributed and more skewed with a larger standard deviation and a higher degree of dispersion.

3.1. The spatial distribution characteristics and the mechanisms

To analyze the spatial distribution of fog days in Shandong Province during 2008–2019, this study used the Cressman interpolation method to interpolate the statistical station data to a latitude and longitude grid with a spatial resolution of 0.1°×0.1°; accordingly, the distributions of the numbers of total fog, light fog, dense fog, and extreme fog days were obtained (Fig. 3). Because the altitude of Taishan station is 1533.7 m, almost within the cloud layer, most of the fog observed at this station may be low clouds. The observation data showed a high frequency of extreme fog days at this station; however, the formation mechanism of this low visibility differed from other regions. Therefore, the Taishan station was excluded from the analyses of the spatiotemporal distribution of fog. For the spatial distribution of fog in Shandong province, a few fog days region appeared a northeast-southwest trending zone in the central region, where was higher altitude topography, and more fog days on both sides can be found at lower altitude areas (Fig. 1 and Fig. 3). A few total fog days region located in the central region in Shandong province were about 130 days in the 12 years from 2008 to 2019, including the light fog of about 50 days (Fig. 3b). The numbers of total fog located in the west of Shandong province reached about 340 days,

which included about 80 dense fog days and 140 extreme fog days (Figs. 3c and d). The coastal stations in eastern Shandong (such as Chengshantou and Shidao) reported high numbers of fog days (Fig. 3a), especially extreme fog days (Fig. 3d), which might be related to the adjacent ocean (Huang et al. 2011; Choi 2013; Pithani et al. 2019; Tian et al. 2020).

Shandong features unique terrain, and the elevation of central Shandong (Taishan Mountains) is higher than those of the surrounding areas, and the spatial distribution characteristics of fog in Shandong Province showed that the higher-elevation area in the center of the study area corresponded to low numbers of total fog, light fog, dense fog, and extreme fog days, and the lower-elevation areas on both sides exhibited high numbers (Fig. 1 and Fig. 3), which indicates that the formation of fog in Shandong Province might be related to the terrain (Fu et al. 2014).

On the other hand, the formation of fog requires a nearly saturated or supersaturated water vapor environment, which necessitates favorable meteorological conditions. Figure 4 shows the box-whisker plot of the average daily average RH and DTR at low-altitude (< 100 m) stations and high-altitude (> 100 m) stations (excluding Taishan station). The daily average RH was present on 65.0% at low-altitude stations and 62.5% at high-altitude stations (Fig. 4a). DTR was present on 9.7°C at low-altitude stations and 9.4°C at high-altitude stations (Fig. 4b). Compared with high altitude areas, low altitude areas had more abundant water vapor conditions and larger DTR, which was more conducive to the formation of fog in low altitude areas.

To quantify the respective effects of altitude, background RH, and DTR on the spatial distribution of fog frequency, the method from Liu et al. (2017) and Sharma et al. (2019) was used. Therefore, multivariate linear regression was established:

$$F = d + ax_1 + bx_2 + cx_3 \quad (1)$$

where *a*, *b*, and *c* are regression coefficients, and *d* is constant. *F* is fog days, and x_1, x_2, and x_3 indicate altitude, background RH, and DTR of meteorological stations, respectively.

Then, the relative effects of the three factors are as follows:

$$F_1 = a\Delta x_1/(E) \times 100\%, F_2 = b\Delta x_2/(E) \times 100\%, F_3 = c\Delta x_3/(E) \times 100\% \quad (2)$$

where Δ is the standard deviation and $E = |a\Delta x_1| + |b\Delta x_2| + |c\Delta x_3|$. In this way, the relative effects of three factors on the spatial distribution of fog frequency can be obtained.

The relative effects of the altitude, daily average RH, and DTR on the spatial distribution of fog were calculated in Table 1. The altitude had negative relative effects on the spatial distribution of fog days, while daily average RH and DTR had positive relative effects. Specifically, daily average RH was the dominant factor among the three factors on the spatial distribution of fog, which accounted for approximately 61.95% in total fog, 44.24% in light fog, 69.07% in dense fog, and 72.57% in extreme fog. And the relative effect of RH on its spatial distribution became more important with increasing fog levels.

Altitude was the factor that accounted for approximately − 19.68% in total fog, -15.89% in light fog, -19.89% in dense fog, and − 22.64% in extreme fog, which means that high level fog corresponded to a relatively larger negative relative effect of altitude. With the enhancement of the level of fog, the effect of the DTR on the spatial distribution of fog days decreased, which accounted for approximately 39.87% in light fog, 11.04% in dense fog, and 4.79% in extreme fog. These indicated that the relatively low altitude, high daily average RH, and high DTR correspond to the high-frequency area of fog days, and these factors had different relative effects on the spatial distributions of different levels of fog.

Table 1
Relative effects (%) of altitude (F1), RH (F2), and DTR (F3) on the spatial distribution of fog (total, light, dense, and extreme fog) days in Shandong Province.

Classification	Light fog	Dense fog	Extreme fog	Total fog
F1	-15.89	-19.89	-22.64	-19.68
F2	44.24	69.07	72.57	61.95
F3	39.87	11.04	4.79	18.37

Under the influence of the uneven terrain, the development of the wind and water vapor field often determines the location and time of fog formation (Golding 1993; Walmsley et al. 1996). A comparison between fog days and non-fog days reveals that the wind field in central Shandong was a divergent anticyclone on non-fog days that passed through southern and western Shandong and then flowed from northern Shandong to the Bohai Sea; namely, the airflow flowed from the mainland to the Yellow Sea (Fig. 5b). Figure 5d shows that the water vapor flux was relatively small on non-fog days in Shandong Province, and there was no water vapor transport channel, so no water vapor convergence occurred in the whole area. In addition, for the entire study area, the wind speed on non-fog days was greater than that on fog days, which was not conducive to the formation of stable atmospheric stratification. Under these conditions, the water vapor in the whole region on non-fog days was far less than that on fog days (Figs. 5a and b), and these meteorological conditions were not conducive to fog formation in this area.

However, on foggy days, the northerly wind originating from the Bohai Sea was divided into two branches under the influence of the terrain (Fig. 5c). The first airflow flowed to the west of Shandong, whereas the second airflow flowed to the eastern sea area of the Shandong Peninsula, then flowed through the Yellow Sea to southern Shandong in the form of an anticyclone and finally turned southeasterly. Figure 5c shows that southern Shandong Province exhibited high water vapor flux, namely, a strong water vapor transport belt. Sufficient water vapor conditions were conducive to the formation of fog in southern Shandong and coastal areas. The second airflow carrying warm and humid air from the Yellow Sea along this water vapor transport channel, northeasterly cold air (the first airflow) from the Bohai Sea, and westerly (or northwesterly) wind from the foot of the Taihang Mountains converged along a line in

western Shandong Province. The area corresponding to this convergence line was characterized by negative water vapor flux divergence (Fig. 5e); namely, water vapor converged in this area. Therefore, the second airflow carried water vapor to eastern Shandong Province, and water vapor accumulated under the convergence of the wind field. In addition, many studies have shown that the convergence of cold and warm winds easily forms frontal fog (Tardif and Rasmussen 2008, 2010; Guo and Guo 2016). Therefore, such wind field and water vapor conditions under terrain conditions were conducive to the formation of fog in western Shandong Province, constituting one of the reasons for the frequent occurrence of fog in this region. In the Taishan Mountains in central Shandong Province, the wind field was divergent, the water vapor flux was small, and the divergence of the water vapor flux was positive; namely, water vapor divergence occurred (Fig. 5e). Hence, the low water vapor caused by the wind field under the terrain was beneficial to form low-frequency fog in this area.

3.2. Interannual variation and distribution of fog and its impact factors

The numbers of fog days at each station in 2008–2019 were linearly fitted, and the annual change rates of total fog, light fog, dense fog, and extreme fog days were obtained. Overall, 88.5% of all stations in Shandong Province showed an increasing trend of total fog days; a greater increase was in the western region, where Chiping station had the fastest growth (6.1 d a^{-1} (d a^{-1} stands day $year^{-1}$)). The number of fog days in most central stations experienced slow growth, and only a few stations in the eastern coastal region had slight decreasing trends (Fig. 6a). Light fog was the main contributor to fog growth. Approximately 75.2% of all stations showed an increasing trend of light fog days. The growth rate in the western region was larger than that in the eastern region overall, and the fastest growth rate was observed at Guangrao station (3.1 d a^{-1}) (Fig. 6b). For dense fog, 68.0% of the stations displayed an increasing trend, and the fastest growth occurred at Linqing station (1.5 d a^{-1}). Thirty-two percent of the stations had a decreasing trend, and most of them were distributed in the coastal and central areas; among them, Shidao station (-1.4 d a^{-1}) had the fastest decline (Fig. 6c). For extreme fog, 67.9% of the stations reported an increasing trend; almost all the stations in the western region experienced increasing trends, some of which were growing rapidly, and Chiping station (3.2 d a^{-1}) reported the fastest growth rate. In contrast, the stations with decreasing trends were distributed in the central, southern, and coastal areas, and the station with the fastest decline was Chengshantou station (-3.0 d a^{-1}) (Fig. 6d). It should be pointed out that more than half of the stations passed the significance test of 5%. In addition, the haze days presented an increasing trend, which indicated that the air pollution in Shandong has been aggravating in recent years. The haze days increased at most sites, and the distribution of the growth rate of haze days was basically consistent with that of fog days (Fig. 6e). The growth rate of haze days at the western stations was also greater than that at the eastern stations. This shows that the background of aggravating air pollution may be an important factor for the gradual increase in the frequency of fog.

From 2008 to 2019, the trends of the spatially averaged annual numbers of total fog, light fog, dense fog, and extreme fog days in Shandong Province were similar and could be divided into three stages (Figs. 7a

and b). The first stage was 2008–2012, during which the spatially averaged number of fog days remained relatively unchanged with a slight decrease over time; this stage had the fewest annual numbers of fog days during the whole research period. The spatially averaged annual occurrences of light fog and dense fog were maintained at approximately 4 days, that of extreme fog was maintained at approximately 6 days and slightly decreased, and that of total fog occurred approximately 13 days with a slightly decreasing trend (Fig. 7a). The slope of the linear fit of the corresponding spatially averaged 3-year moving average in this stage was approximately 0 (Fig. 7b). The second stage was 2012–2016, during which the spatially averaged annual number of fog days increased rapidly. The number of total fog days increased by 125% from 12 days in 2012 to 27 days in 2016, and the number of light fog days increased by 125% from 4 days in 2012 to 9 days in 2016; in contrast, the numbers of dense and extreme fog days increased relatively slowly by 50% and 100%, respectively, from 4 to 6 days and 5 to 10 days. The slope corresponding to the 3-year moving average linear fitting in this stage far exceeded 0. The third stage was 2016–2019, during which the spatially averaged annual number of fog days remained constant with a slightly decreasing trend.

Corresponding to the annual variation of fog days, the spatially averaged annual specific humidity at 1000 hPa over Shandong Province also showed an increasing trend from 2008 to 2019 (Figs. 7c and d), while the spatially averaged annual wind speed showed a decreasing trend (Figs. 7e and f). Specific humidity exhibited a strong positive correlation with the number of fog days: the correlation coefficients with the numbers of total fog, light fog, dense fog, and extreme fog days were 0.591*, 0.594*, 0.484, and 0.579*, respectively (the symbol (*) indicates significance at the 5% significance level (two-tailed)), which indicated that the occurrence frequency of fog increased with increasing specific humidity. The specific humidity in 2013–2018 increased significantly compared with that before 2012; this abundance of water vapor during 2013–2018 enabled the increase in fog frequency after 2012. The numbers of total fog, light fog, dense fog, and extreme fog days exhibited negative correlations with the wind speed with coefficients of -0.487, -0.426*, -0.574, and − 0.483, respectively. In particular, the fog frequency increased rapidly with the abrupt decrease of wind speed after 2012, indicating that a lower wind speed was more conducive to the formation of fog. Moreover, the spatially averaged annual variation of haze days showed an increasing trend (Figs. 7g and h), which had a strong positive correlation with total fog, light fog, dense fog, and extreme fog days, and the correlation coefficients were 0.867**, 0.885**, 0.717**, and 0.826**, respectively (the symbol (**) indicates significance at the 1% significance level (two-tailed)). Therefore, the increase in water vapor, the aggravation in air pollution, and the decrease in wind speed may have been important factors governing the increased fog frequency in Shandong Province during 2008–2019.

Moreover, Figs. 6 and 7 indicate that the growth rate of light fog days was much larger than that of dense fog and extreme fog days, in which the growth rates were produced by the interaction of the specific humidity, wind speed, and air pollution. The meteorological conditions that are conducive to the formation of various types of fog are different (Tang et al. 2009; Wei et al. 2010). Therefore, the responses of variations of different levels of fog days to the changes of meteorological conditions are also different. This needs further detailed study.

3.3. Monthly and seasonal interannual and intra-annual variations in fog

Table 2 demonstrates that in the 12 years from 2008 to 2019, the spatially average numbers of total fog days in Shandong Province in spring (Mar., Apr., and May), summer (Jun., Jul., and Aug.), autumn (Sept., Oct., and Nov.), and winter (Dec., Jan., and Feb.) were 37, 35, 67, and 79, respectively (the spatially annual average in four seasons were 3.1, 2.9, 5.6, and 6.6 days, respectively). More fog days occurred in winter and autumn than in spring and summer. The standard deviations of fog days in summer and autumn were larger than those in spring and winter, and the degree of dispersion in the former two seasons was higher than that in the latter, suggesting a high and concentrated frequency of fog days at the meteorological stations in summer and autumn.

Table 2
Spatial average numbers and standard deviations of total fog, light fog, dense fog, and extreme fog in each season from 2008–2019.

Classification	Spring (Std. Dev.)	Summer (Std. Dev.)	Autumn (Std. Dev.)	Winter (Std. Dev.)
Light fog	11 (7)	13 (11)	24 (16)	27 (12)
Dense fog	10 (10)	10 (12)	16 (10)	18 (9)
Extreme fog	16 (20)	11 (30)	28 (20)	35 (16)
Total fog	37 (31)	35 (44)	67 (41)	79 (31)

The monthly and seasonal interannual variations in fog in Shandong Province during 2008–2019 were further analyzed. In general, the overall frequency of fog in Shandong Province in autumn and winter was higher than that in spring and summer during 2008–2019 (Fig. 8a). Specifically, the distribution of light fog in each season was almost consistent with the distribution of total fog (Fig. 8b). The seasonal frequency distributions of dense fog and extreme fog were slightly different from those of total fog and light fog but were also similarly higher in autumn and winter than in spring and summer (Figs. 8c and d). Except for summer, the frequency of dense fog and extreme fog increased in other seasons over the study period. The frequency increased the fastest in winter for different levels of fog. The frequency of light fog remained nearly unchanged in all seasons from 2008 to 2012 and began to increase rapidly after 2012, but the frequency fell rapidly in spring, summer, and autumn after 2017. In contrast, the frequency of light fog in winter increased rapidly after 2017 (Fig. 8b). Dense fog and extreme fog displayed similar trends. The difference was that the frequency of dense fog in autumn was the highest during 2015–2018, and in winter, it fell rapidly after 2014 (Figs. 8c and d). All levels of fog had high frequencies in Nov., Dec., and Jan., followed by Jul.-Oct. The frequency of fog increased nearly every month over the study period;

among the three levels of fog, light fog was the main contributor to the increase in total fog frequency. The months with the highest frequency of total fog, light fog, dense fog, and extreme fog were Dec. 2015, Dec. 2015, Dec. 2015, and Jan. 2013, respectively (Figs. 8e-h).

In order to further analyze the reason for the higher fog frequency in autumn and winter, we calculated the spatial average lower-tropospheric stability (LTS). The LTS reflects the strength of the inversion, which is the difference in potential temperature at 700 hPa and the surface (LTS = θ_{700} - θ_0, Klein and Hartmann 1993; Wood and Hartmann 2006; Zhang et al. 2010). In this way, the strength of the inversion of each month and season was captured.

Figure 9 shows the spatial average LTS of spring, summer, autumn, winter, and each month in Shandong Province from 2008 to 2019. It can be seen that LTS had a distinct seasonal cycle. The LTS in autumn and winter was greater than that in spring and summer, which indicated that during autumn and winter, the boundary layer tends to form a stronger low-level temperature inversion than that in spring and summer. It was obvious that the seasonal cycles of fog frequency and LTS were generally in phase, which illustrated that the fog frequency was high when LTS was large, while low when LTS was small (Figs. 8 and 9). Inversion is conducive to the formation of fog because it stabilizes the lower atmosphere (Liu et al. 2012; Liu et al. 2016). Therefore, the stronger inversion in autumn and winter formed a favorable low-level atmospheric stability condition for frequent fog. Moreover, the statistical results also show that the temporal-spatial average wind speeds at 1000 hPa in spring, summer, autumn, and winter in Shandong from 2008 to 2019 were 1.35 m/s, 1.27 m/s, 1.22 m/s, and 1.18 m/s, respectively, revealing that the wind speed in autumn and winter was smaller than that in spring and summer.

3.4. Diurnal variation and duration of fog

Statistical analyses were conducted on the frequency of total fog, light fog, dense fog, and extreme fog at each time point, the start time point of fog, and the end time point of fog over the day at the 122 meteorological stations in Shandong Province during 2016–2019. It was found that foggy weather in Shandong Province can occur at any time of the day, with fog frequently occurring from 00:00 to 08:00 (Fig. 10a) (Note: All the time in this paper is provided in China Standard Time, CST). The frequencies of light fog, dense fog, and extreme fog in this period accounted for 66.8%, 64.8%, and 70.8% in one day, respectively, all peaking at 06:00 (accounting for 9.1%, 9.7%, and 10.1%, respectively). The minimum frequencies of different levels of fog were reached at 15:00 (accounting for 0.9%, 0.9%, and 0.6%, respectively). Near this time, the temperature was typically very high (Fig. 10a), and the supersaturation required for fog formation was difficult to achieve, hindering the formation of fog. Figure 10a shows that the temperature gradually decreased from 15:00 to approximately 06:00 the next day. Low temperature at night creates the condition for the surface air to become saturated, allowing water vapor to condense and form fog (Belorid et al. 2015; Bari et al. 2016); therefore, the proportion of fog gradually increased during this period. After sunrise, the temperature gradually rose, and the fog began to dissipate slowly. From 08:00 to 14:00, the temperature increased sharply and then reached the maximum temperature (Fig. 10a), so most of the fog tended to dissipate during this period. The daily cycles of fog frequency and

temperature were generally reversed, which indicated that the diurnal variation in temperature may be responsible for the diurnal variation in fog frequency.

In Shandong Province, the start time concentrated mainly from night to the early morning, peaking at 05:00 (Fig. 10b), and the end time also concentrated primarily from night to morning, peaking at 06:00–07:00 (Fig. 10c). The diurnal variations of the start and end times of the different levels of fog were similar, and the end time was pushed forward by 1–3 h compared to the start time, indicating that the duration of fog was mainly 1–3 h.

According to the statistics of the fog duration, the duration of most fog events was 1 h in Shandong Province, with the frequency of this period accounting for 50.9%. The proportions of fog duration of 1–3 h, 4–6 h, 7–9 h, 10–12 h, 13–24 h, and 25 h and above were 69.0%, 13.7%, 7.0%, 4.0%, 4.8%, and 1.5%, respectively. The fog duration in Shandong Province was mainly between 1–3 h, but fog days still occurred with durations exceeding 12 h or even 24 h (Fig. 11).

4. Discussion And Conclusions

In this paper, the spatiotemporal distribution characteristics and variations of fog and its impact factors in Shandong Province, China in recent years were investigated by using diverse meteorological data. The main conclusions were summarized as follows:

(1) The spatial distribution of fog in Shandong province was consistent with the topographic characteristics, and a few fog days region appeared a northeast-southwest trending zone in the central region, where was higher altitude topography, and more fog days on both sides can be found at lower altitude areas. Due to the effect of the topography, the characteristics of water vapor transport and convergence played important roles in the spatial distribution of fog days. The quantitative relative effects of the daily average RH, DTR, and the altitude on the spatial distribution of fog days indicated that daily average RH was a dominant factor among the three factors for the spatial distribution of fog days, and RH and DTR had positive relative effects, while altitude had a negative relative effect. The relative effect of RH and altitude became more important with increasing fog level, while that of DTR became less important with increasing fog level. Therefore, the characteristics of water vapor transport and convergence and the spatial difference in the RH and DTR under special terrain conditions determined the characteristics of the spatial distribution of fog days in Shandong Province.

(2) The annual number of fog days of different levels (light fog, dense fog, and extreme fog) in Shandong Province from 2008 to 2019 showed an increasing trend. It can be roughly divided into three stages: a stage of constant or slightly declining numbers from 2008 to 2012, a stage of rapidly increasing numbers from 2012 to 2016, and another stage of constant or slightly declining numbers from 2016 to 2019. The growth rate of western stations was higher than that of eastern stations. The increase in water vapor, the aggravation in air pollution, and the decrease in wind speed have been important factors governing the increased fog frequency in Shandong Province during 2008–2019.

(3) The seasonal frequencies of fog in Shandong Province during 2008–2019 decreased in the order of winter, autumn, spring, and summer. The seasonal variations of the different levels of fog were similar, and the frequency of fog increased in all seasons; the frequency of fog increased the fastest in winter. The monthly average occurrence frequencies of the different levels of fog were high in November, December, and January, followed by July-October. The reasons why the fog frequency in autumn and winter was higher than that in spring and summer were related to the greater value of LTS and the lower wind speed at the lower levels.

(4) Fog occurred frequently within 00:00–08:00 during 2016–2019 in Shandong Province. During this period, light fog, dense fog, and extreme fog accounted for 66.8%, 64.8%, and 70.8% in one day, respectively, all reaching their peaks at 06:00. The frequencies of different levels of fog reached their minima at 15:00. The diurnal variation in temperature was responsible for the diurnal variation in fog frequency. The start time of fog peaked at 05:00, and the end time peaked at 06:00–07:00. The durations of most fog were 1–3 h, accounting for 69.0%.

Many studies have shown that the fog frequency over China, Europe, and some other countries had been declining over the past few decades (van Oldenborgh et al. 2010; Ladochy and Witiw 2011; Ding and Liu 2014; Akimoto and Kusaka 2015). However, our research results showed that the fog frequency in Shandong Province of China has increased rapidly in the past 12 years from 2008 to 2019. This was a very interesting conclusion, which indicated that in the region where the fog frequency showed a decreasing trend in a large-scale range, the local fog frequency may show an increasing trend was a very beloved phenomenon worthy of attention. This paper only carried out a comprehensive statistical analysis of different levels of fog in Shandong Province. In the future, more kinds of data can be applied to analyze the temporal and spatial distribution characteristics of specific types of fog (such as radiation fog, advection fog, evaporation fog, frontal fog, and precipitation fog) more specifically, which is also an interesting research direction. The results of this study can be used as a basis for further research of fog in Shandong Province. In addition, the conclusions of spatial, seasonal, and diurnal distribution characteristics can provide certain references for the location and operation time of the work of artificial dissipating fog. Moreover, this research can also serve as a helpful reference for traffic and airport safety management and control in Shandong Province.

Declarations

Funding This research was supported in part by the National Key Research and Development Plans of China (Grant Nos. 2019YFC1510304, 2016YFE0201900-02) and the National Natural Science Foundation of China (Grant No. 41575037).

Conflict of interest The authors declare no competing interests.

Ethics approval The authors declare there are no ethical issues involved.

Consent to participate All authors contributed to the study's conception and design. All authors commented on previous versions of the manuscript and read and approved the final manuscript.

Consent for publication The authors agree to publication in Theoretical and Applied Climatology.

Data Availability The surface meteorological station data are available from China National Meteorological Data Center (http://data.cma.cn/en/). ERA5 reanalysis data are available from European Centre for Medium-Range Weather Forecasts (https://www.ecmwf.int/).

Code availability Not applicable

Authors' contributions The study was jointly designed by Weixi Shu, Hui Xiao, and Danhong Fu; Bingsong Chang was responsible for processing and analyzing data; Weixi Shu wrote the first draft with input from all co-authors, Danhong Fu, Qiang Feng, Shujing Shen, and Huiling Yang provided all technical support for the data analysis and contributed to the writing. All authors read and approved the final manuscript.

References

1. Akimoto Y, Kusaka H (2015) A climatological study of fog in Japan based on event data. Atmos Res 151:200-211. https://doi.org/10.1016/j.atmosres.2014.04.003.
2. Bari D, Bergot T, Khlifi MEl (2016) Local meteorological and large-scale weather characteristics of fog over the Grand Casablanca region, Morocco. J Appl Meteor Climatol 55(8):1731-1745. https://doi.org/10.1175/JAMC-D-15-0314.1.
3. Bartok J, Bott A, Gera M (2012) Fog prediction for road traffic safety in a coastal desert region. Bound-Layer Meteor 145(3):485-506. https://doi.org/10.1007/s10546-012-9750-5.
4. Belorid M, Lee CB, Kim JC, Cheon TH (2015) Distribution and long-term trends in various fog types over South Korea. Theor Appl Climatol 122(3-4):699-710. https://doi.org/10.1007/s00704-014-1321-x.
5. Chen SY, Yan Y, Liu G, Fang DX, Wu Z, He J, Tang JP (2019) Spatiotemporal characteristics of precipitation diurnal variations in Chongqing with complex terrain. Theor Appl Climatol 137(1-2):1217-1231. https://doi.org/10.1007/s00704-018-2662-7.
6. Choi H (2013) Sea fog by southerly warm air over cool sea waters of the Southward North Korea cold current along the Korean East Coast under cyclogenesis in the Yellow Sea. Disaster Advances 6(5):41-53. https://doi.org/10.1007/s10519-013-9590-1.
7. Cressman GP (1959) An operational objective analysis system. Mon Wea Rev 87(10): 367-374. https://doi.org/10.1175/1520-0493(1959)0872.0.CO;2.
8. Ding YH, Liu YJ (2014) Analysis of long-term variations of fog and haze in China in recent 50 years and their relations with atmospheric humidity. Science China Earth Sciences 57(1):3646. https://doi.org/10.1007/s11430-013-4792-1.

9. Doyle M, Dorling S (2002) Visibility trends in the UK 1950–1997. Atmos Environ 36(19):3161-3172. https://doi.org/10.1016/S1352-2310(02)00248-0.
10. Fu GQ, Xu WY, Yang RF, Li JB, Zhao CS (2014) The distribution and trends of fog and haze in the North China Plain over the past 30 years. Atmos Chem Phys 14(21):11949-11958. https://doi.org/10.5194/acp-14-11949-2014.
11. Fu G, Guo JT, Xie SP, Duane YH, Zhang MG (2006) Analysis and high-resolution modeling of a dense sea fog event over the Yellow Sea. Atmos Res 81(4):293-303. https://doi.org/10.1016/j.atmosres.2006.01.005.
12. Fu Q, Zhang YT, Li TX, Cui S, Liu D (2018): Spatiotemporal complexity analysis of daily precipitation in a Changing environment in Heilongjiang Province, China. J Hydrol Eng 23(11). https://doi.org/10.1061/(ASCE)HE.1943-5584.0001703.
13. Golding BW (1993) A study of the influence of terrain on fog development. Mon Wea Rev 121(9):2529-2541. https://doi.org/10.1175/1520-0493(1993)121<2529: ASOTIO>2.0.CO;2.
14. Guo LJ, Guo XL (2016) The type, vertical structure and physical formation mechanism of persistent heavy fog events during 2009-2013 in the Beijing Region. Chinese J Atmos Sci 40(02):296-310. https://doi.org/10.3878/j.issn.1006-9895.1505.14275. (in Chinese)
15. Huang H J, Liu HN, Jiang WM, Huang J, Mao WK (2011) Characteristics of the boundary layer structure of sea fog on the coast of Southern China. Adv Atmos Sci 28(6):1377-1389. https://doi.org/10.1007/s00376-011-0191-8.
16. Hunova I, Brabec M, Maly M, Valerianova A (2019) Long-term trends in fog occurrence in the Czech Republic, Central Europe. Sci Total Environ 711:135018. https://doi.org/10.1016/j.scitotenv.2019.135018.
17. Jenamani RK (2012) Micro-climatic study and trend analysis of fog characteristics at IGI airport New Delhi using hourly data (1981-2005). Mausam 63(2):203-218.
18. Kim W, Yum SS, Kim CK (2020) Numerical simulation of sea fog over the Yellow Sea: Comparison between UM + PAFOG and WRF + PAFOG coupled systems. Asia-pac J Atmos Sci 56(1):89-105. https://doi.org/10.1007/s13143-019-00134-9.
19. Klein SA, Hartmann DL (1993) The seasonal cycle of low stratiform clouds. J Climate 6(8):1587-1606. https://doi.org/10.1175/1520-0442(1993)006<1587:tscols>2.0.co;2.
20. Ladochy S, Witiw M (2011) The continued reduction in dense fog in the Southern California region: Possible causes. Pure Appl Geophys 169(5):1157-1163. https://doi.org/10.1007/s00024-011-0366-3.
21. Lange CA, Matschullat J, Zimmermann F, Sterzik G, Wienhaus O (2003) Fog frequency and chemical composition of fog water-a relevant contribution to atmospheric deposition in the Eastern Erzgebirge, Germany. Atmos Environ 37(26):3731-3739. https://doi.org/10.1016/S1352-2310(03)00350-9.
22. Li SH, Sun XJ, Zhang RW, Zhang CL (2019) A feasibility study of simulating the Micro-Scale wind field for wind energy applications by NWP/CFD model with improved coupling method and data assimilation. Energies 12(13):2549. https://doi.org/10.3390/en12132549.

23. Liu DY, Niu SJ, Yang J, Zhao LJ, Lu JJ, Lu CS (2012) Summary of a 4-Year Fog field study in Northern Nanjing, Part 1: Fog boundary layer. Pure Appl Geophys 169:5-6. https://doi.org/10.1007/s00024-011-0343-x.
24. Liu DY, Yan WL, Yang J, Pu MJ, Niu SJ, Li ZH (2016) A study of the physical processes of an advection fog boundary layer. Bound-Layer Meteor 158(1):125-138. https://doi.org/10.1007/s10546-015-0076-y.
25. Liu Q, Sheng LF, Cao ZQ, Diao YN, Wang WC, Zhou Y (2017) Dual effects of the winter monsoon on haze-fog variations in eastern China. J Geophys Res 122(11):5857-5869. https://doi.org/10.1002/2016JD026296.
26. Liu XM, Zhang HZ, Li QX, Zhu YJ (2005) Preliminary research on the climatic characteristics and change of fog in China. J Appl Meteor Sci 16(2). https://doi.org/10.11898/1001-7313.20050210. (in Chinese)
27. Ma Y, Huang R, Chen S, Guo LN (2015) Characteristics of fogs and air quality and their relationship in Qingdao. Meteor Sci Technol 43(05):925-931. (in Chinese)
28. Meyer MB, Lala GG (1990) Climatological aspects of radiation fog occurrence at Albany, New York, J Climate 3(5):577-586. https://doi.org/10.1175/1520-0442 (1990)003<0577:CAORFO>2.0.CO;2.
29. Niu SJ, Lu CS, Yu HY, Zhao LJ, Lu JJ (2010a) Fog research in China: An overview. Adv Atmo Sci 27(3):639-662. https://doi.org/10.1007/s00376-009-8174-8.
30. Niu F, Li ZQ, Li C, Lee HK, Wang MY (2010b) Increase of wintertime fog in China: Potential impacts of weakening of the Eastern Asian monsoon circulation and increasing aerosol loading. J Geophys Res 115. https://doi.org/10.1029/2009JD013-484.
31. Peace RL (1969) Heavy-fog regions in the conterminous United States. Mon Weather Rev 97(2):116-123. https://doi.org/10.1175/1520-0493(1969)0972.3.CO;2.
32. Pithani P, Ghude SD, Prabhakaran T, Karipot A, Hazra A, Kulkarni R, Chowdhuri S, Resmi EA, Konwar M, Murugavel P, Safai PP, Chate DM, Tiwari Y, Jenamani RK, Rajeevan M (2019) WRF model sensitivity to choice of PBL and microphysics parameterization for an advection fog event at Barkachha, rural site in the Indo-Gangetic basin, India. Theor Appl Climatol 136(3-4):1099-1113. https://doi.org/10.1007/s00704-018-2530-5.
33. Qiu JH, Chen HB (2005) Atmospheric physics and atmospheric exploration. China Meteorological Press, 179pp. (in Chinese)
34. Quan J, Zhang Q, He H, Liu J, Huang M, Jin H (2011) Analysis of the formation of fog and haze in North China Plain (NCP). Atmos Chem Phys 11(15):8205-8214. https://doi.org/10.5194/acp-11-8205-2011.
35. Roach WT (1994) Back to basics: Fog: Part 1-Definitions and basic physics. Weather 49(12):411-415. https://doi.org/10.1002/j.1477-8696.1994.tb05962.x.
36. Safai PD, Ghude S, Pithani P, Varpe S, Kulkarni R, Todekar K, Tiwari S, Chate DM, Prabhakaran T, Jenamani RK, Rajeevan MN (2019) Two-Way relationship between aerosols and fog: A case study at IGI airport, New Delhi. Aerosol Air Qual Res 19(1):71-79. https://doi.org/10.4209/aaqr.2017.11.0542.

37. Schichtel BA, Husar RB, Falke SR, Wilson WE (2001) Haze trends over the United States, 1980-1995. Atmos Environ 35(30):5205-5210. https://doi.org/10.1016/S1352-2310(01)00317-X.
38. Sharma OP, Kannan N, Cook S, Pokhrel BK, McKenzie C (2019) Analysis of the effects of high precipitation in Texas on Rainfed Sorghum Yields. Water 11(9). https://doi.org/10.3390/w11091920.
39. Shi CN, Roth M, Zhang H, Li ZH (2008) Impacts of urbanization on long-term fog variation in Anhui Province, China. Atmos Environ 42(36):8484-8492. https://doi.org/10.1016/j.atmosenv.2008.08.002.
40. Shrestha S, Moore GA, Peel MC (2018) Trends in winter fog events in the Terai region of Nepal. Agric For Meteorol 259:118-130. https://doi.org/10.1016/j.agrformet. 2018.04.018.
41. Syed FS, Koernich H, Tjernstroem M (2012) On the fog variability over South Asia. Climate Dyn 39(12):2993-3005. https://doi.org/10.1007/s00382-012-1414-0.
42. Tang XY, Luo L, Wang G, Mo Y (2009) Study on spatial and temporal characteristics of fog in Sichuan Province. Plateau Mountain Meteor Res 29(3):60-65. (in Chinese)
43. Tao Y, Wang S, Tian H, Wen HY (2012) Spatial and temporal characteristics and meteorological conditions for fog formation in Anhui Province. Scientia Geographica Sinica 32(3):374-379. https://doi.org/10.13249/j.cnki.sgs.2012.03.017. (in Chinese)
44. Tardif R, Rasmussen RM (2008) Process-oriented analysis of environmental conditions associated with precipitation fog events in the New York City region. J Appl Meteorol Climatol 47(6):1681-1703. https://doi.org/10.1175/2007JAMC1734.1.
45. Tardif R, Rasmussen RM (2010) Evaporation of nonequilibrium raindrops as a fog formation mechanism. J Atmos Sci 67(2):345-364. https://doi.org/10.1175/2009JAS3149.1.
46. Tian M, Wu B G, Huang H, Wang ZY, Zhang WY (2020) The synoptic condition and boundary layer characteristics of coastal fog around the Bohai Sea. Climatic Environ Res 25(2):199-210. (in Chinese)
47. van Oldenborgh GJ, Yiou P, Vautard R (2010) On the roles of circulation and aerosols in the decline of mist and dense fog in Europe over the last 30 years. Atmos Chem Phys 10(10):4597-4609, https://doi.org/10.5194/acp-10-4597-2010.
48. Vautard R, Yiou P, van Oldenborgh GJ (2009) Decline of fog, mist and haze in Europe over the past 30 years. Nat Geosci 2(2):115-119. https://doi.org/10.1038/NGEO414.
49. Walmsley JL, Schemenauer RS, Bridgman HA (1996) A method for estimating the hydrologic input from fog in mountainous terrain. J Appl Meteor 35(12):2237-2249. https://doi.org/10.1175/1520-0450(1996)035<2237:AMFETH>2.0.CO;2.
50. Wang XF, Chen JM (2014) Fog formation in cold season in Ji'nan, China: Case analyses with application of HYSPLIT model. Adv Meteorol 2014:1-8. https://doi.org/10.1155/2014/940956.
51. Wei JS, Zhu WJ, Yan WL, Sun Y, Wu J, Liu JW (2010) Climatic characteristics of fog and its relevant influencing factors over the coastal areas of Jiangsu. Trans Atmos Sci 33(6):680-687. https://doi.org/10.3969/j.issn.1674-7097.2010.06.005. (in Chinese)

52. Witiw MR, Ladochy S (2008) Trends in fog frequencies in the Los Angeles Basin. Atmos Res 87(3-4):293-300. https://doi.org/10.1016/j.atmosres.2007.11.010.
53. WMO (1992) International Meteorological Vocabulary, vol. 182, *Geneva WMO*, 1-276.
54. Wood R, Bretherton CS (2006) On the relationship between stratiform low cloud cover and lower-tropospheric stability. J Climate 19(24):6425-6432. https://doi.org/10.1175/JCLI3988.1.
55. Yang Y, Liao H, Lou S (2016) Increase in winter haze over eastern China in recent decades: Roles of variations in meteorological parameters and anthropogenic emissions. J Geophys Res 121(21):13050-13065. https://doi.org/10.1002/2016JD025136.
56. Ye HC (2009) The influence of air temperature and atmospheric circulation on winter fog frequency over Northern Eurasia. Int J Climatol 29(5):729-734. https://doi.org/10.1002/joc.1741.
57. Zhang SP, Xie SP, Liu QY, Yang YQ, Wang XG, Ren ZP (2009) Seasonal variations of Yellow Sea fog: Observations and Mechanisms. J Climate 22(24):6758-6772. https://doi.org/10.1175/2009JCLI2806.1.
58. Zhang GJ, Vogelmann AM, Jensen MP, Collins WD, Luke EP (2010) Relating satellite-observed cloud properties from MODIS to meteorological conditions for marine boundary layer clouds. J Climate 23(6):1374-1391. https://doi.org/10.1175/2009JCLI2897.1.

Figures

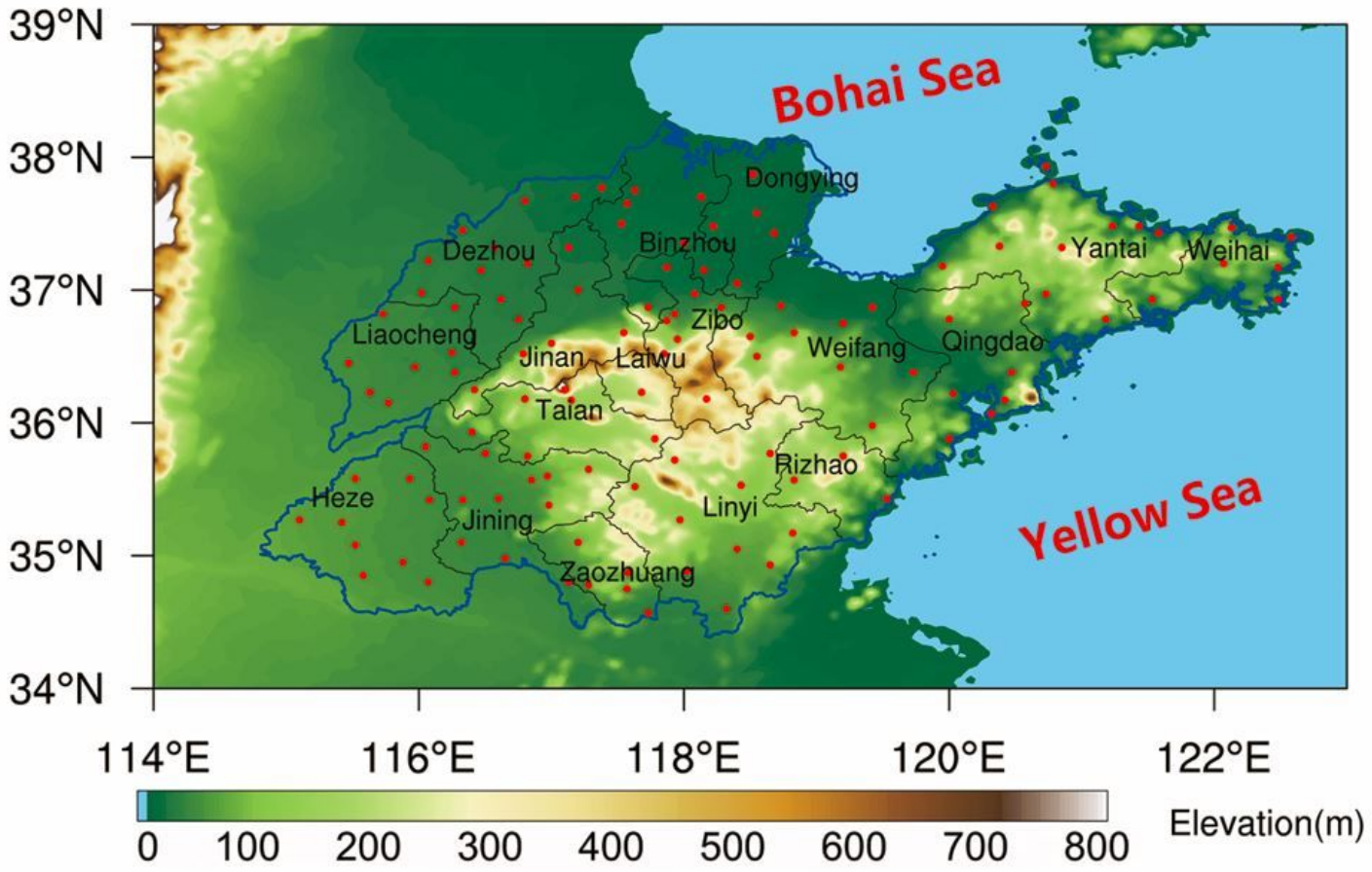

Figure 1

Locations of the measurement sites (red points) in Shandong Province (blue boundary) and the regional topography (color background).

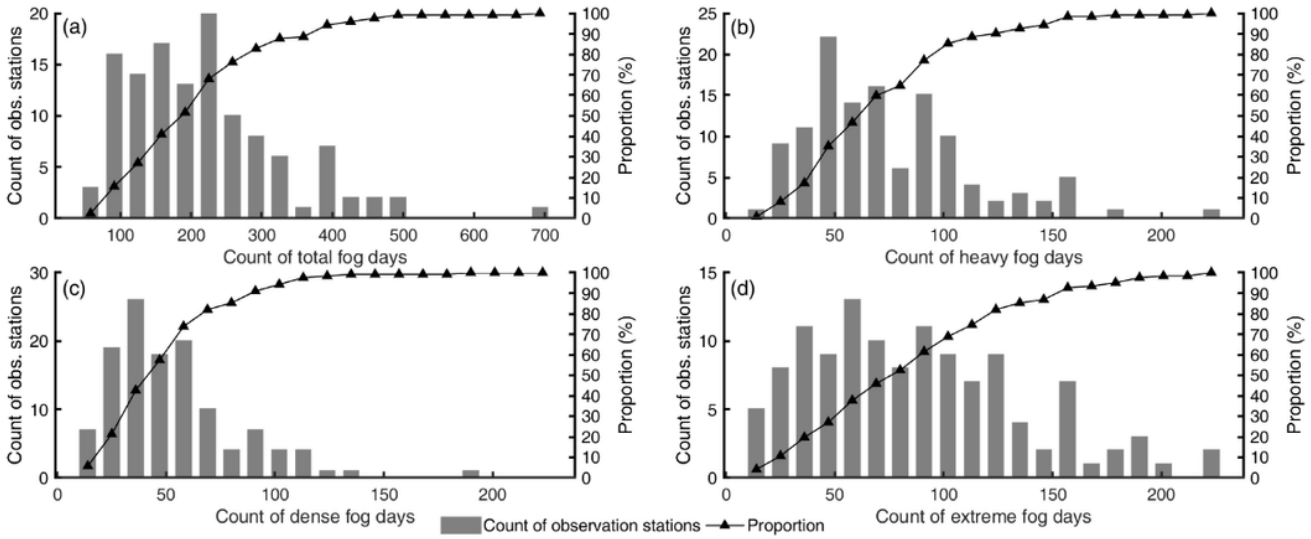

Figure 2

Statistical histograms of the numbers of (a) total fog, (b) light fog, (c) dense fog, and (d) extreme fog days at 122 meteorological stations in Shandong Province from 2008-2019. The black polyline represents the cumulative percentage (%). Among the four plots, (a) total fog takes 52 days as an interval unit, while (b) light fog, (c) dense fog, and (d) extreme fog take 11 days as an interval unit.

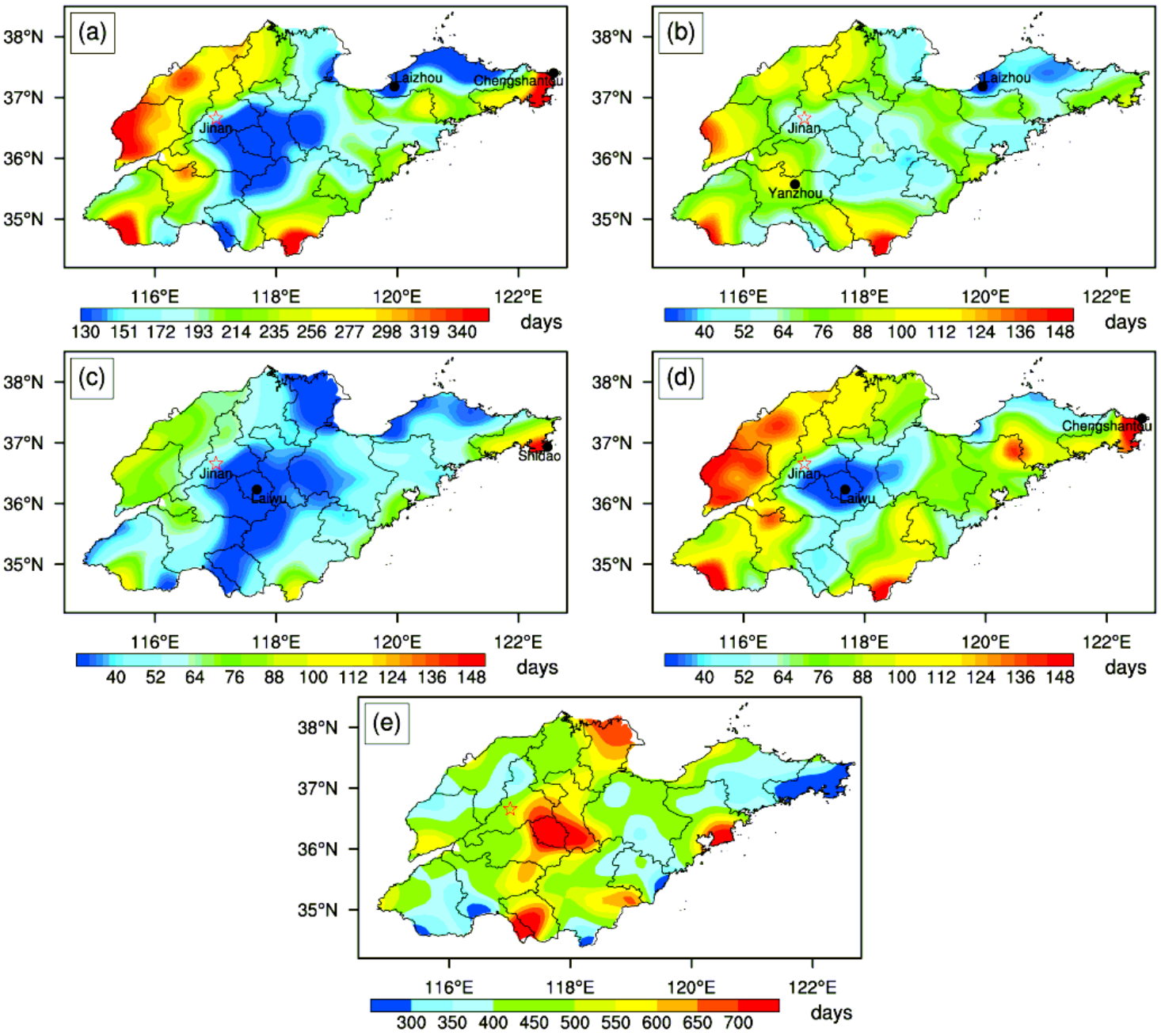

Figure 3

Spatial distributions of the numbers of (a) total fog, (b) light fog, (c) dense fog, and (d) extreme fog in Shandong Province from 2008-2019.

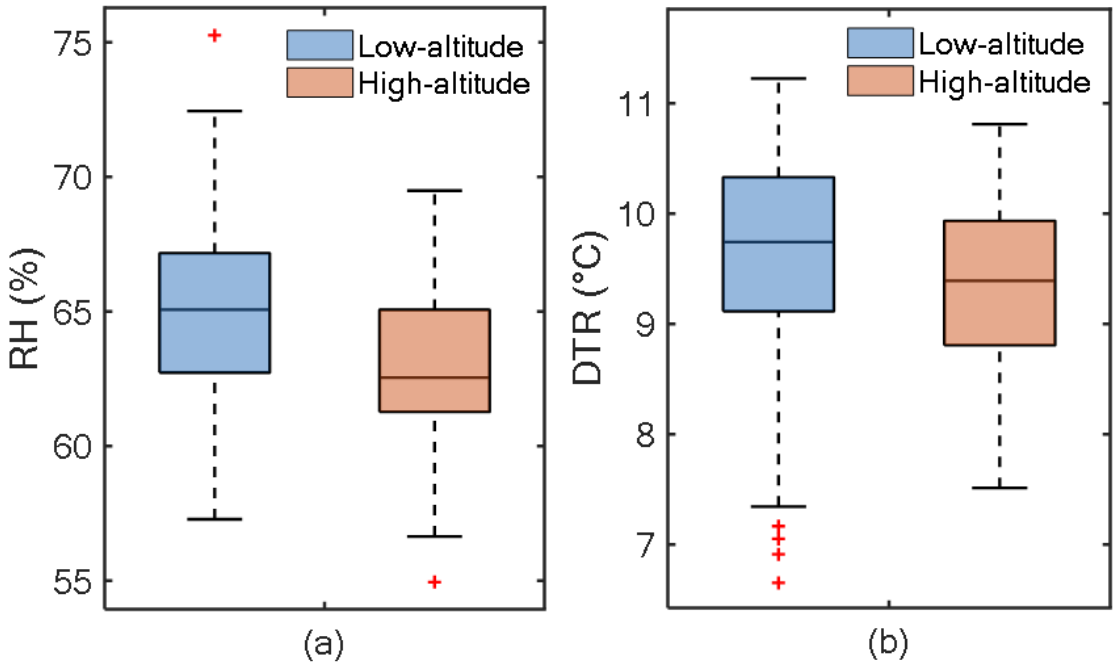

Figure 4

Box-whisker plot of the average (a) daily average RH and (b) DTR at low-altitude (< 100 m) stations and high-altitude (> 100 m) stations during the period 2008-2019.

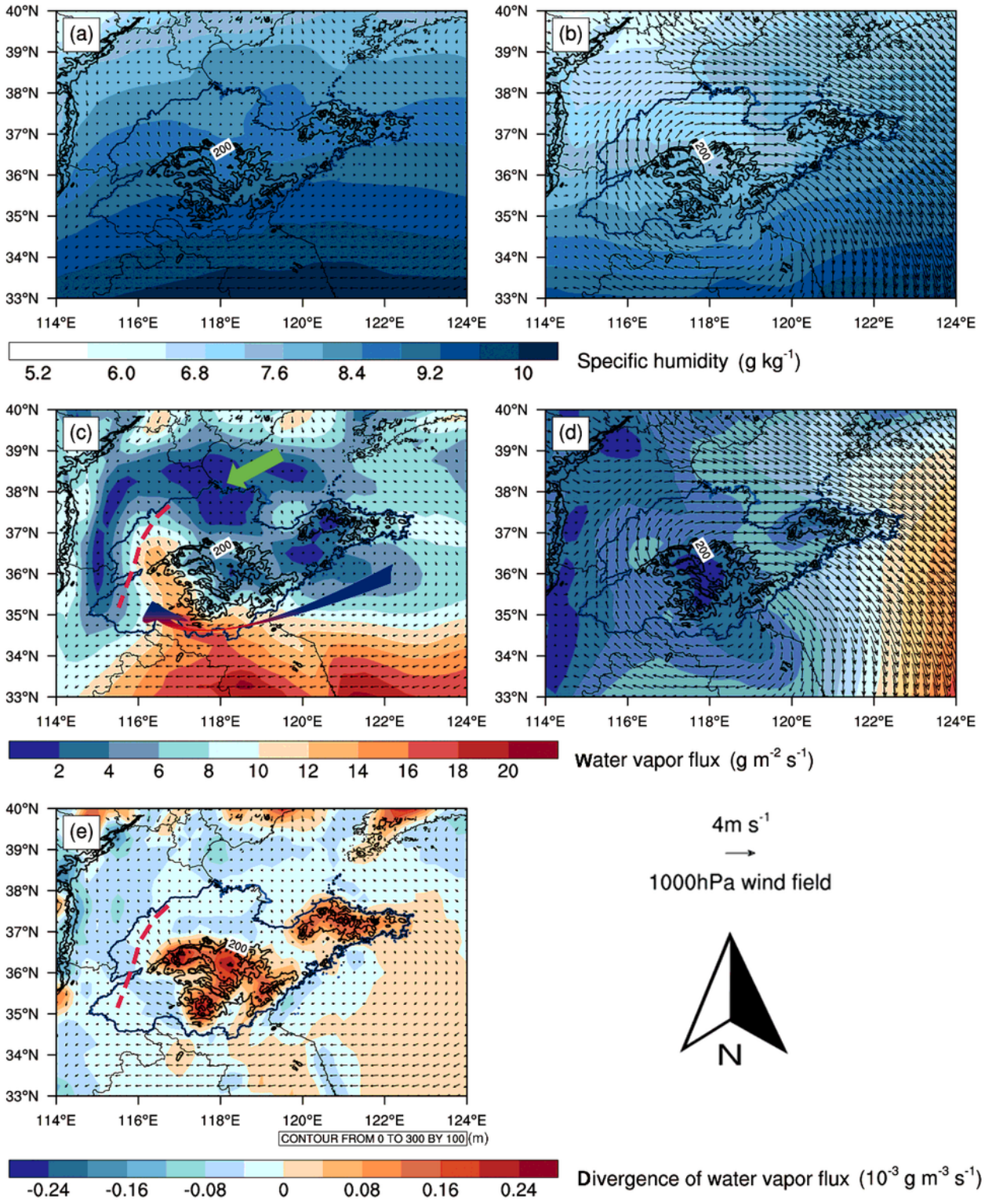

Figure 5

(a) Time-averaged 1000 hPa ERA5 reanalysis wind field (black arrows) and specific humidity distribution (shading) on fog days at 08:00 (Note: All the time in this paper is provided in China Standard Time, CST) from 2008-2019; the blue line delineates the area of study, and the contours represent the terrain of Shandong Province and its surrounding areas. (b) Same as in (a) but for non-fog days. (c) Same as (a) but for the water vapor flux distribution; the thick green arrow represents the first airflow, the thick curved

arrow with a blue-red gradient represents the second airflow, and the thick red dashed line represents the wind field convergence line generated by the terrain. (d) Same as in (c) but for non-fog days. (e) Same as in (c) but for the divergence of the water vapor flux distribution.

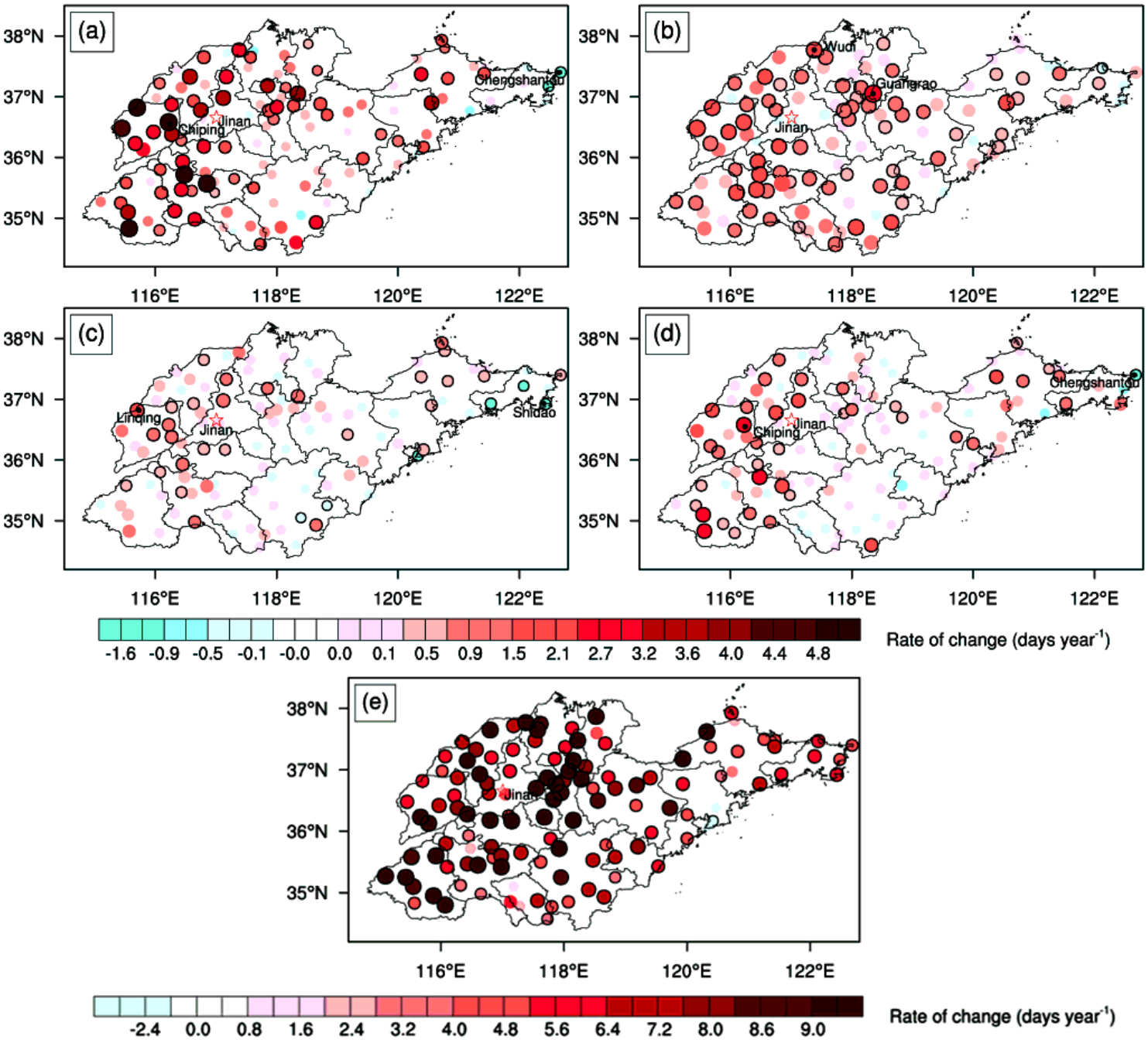

Figure 6

Scatter diagrams of the annual change rates of the numbers of (a) total fog, (b) light fog, (c) dense fog, (d) extreme fog, (e) and haze days at the 122 meteorological stations in Shandong Province from 2008-2019. Colored dots with a black border indicate that the trend is statistically significant at the 0.05 level.

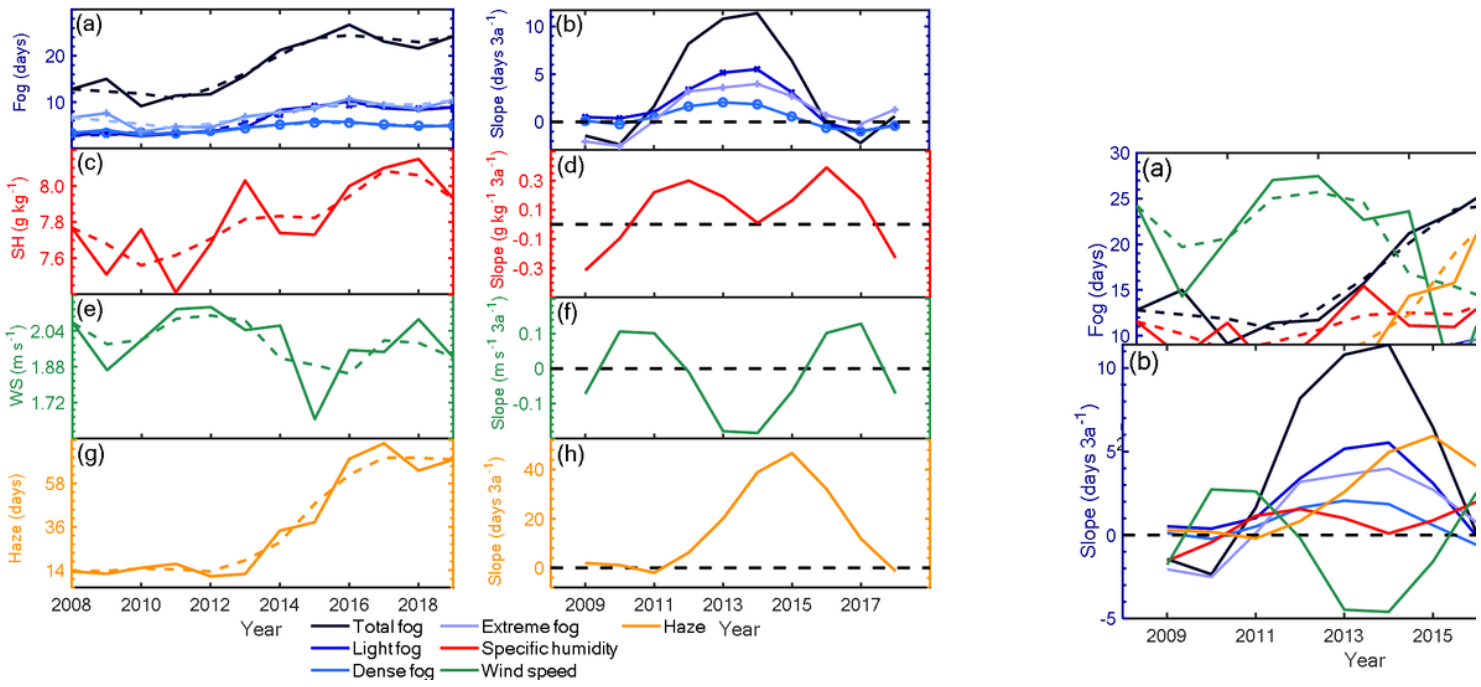

Figure 7

The first column: spatial average annual number (solid line) and 3-year moving average of the number (dashed lines) of (a) fog days (including total fog (blue line), light fog, dense fog, and extreme fog), (c) the 1000 hPa ERA5 specific humidity (red line), (e) wind speed (green line), and (g) haze (orange line) days in Shandong Province from 2008-2019. The second column: same as the first line but is the slope of the 3-year moving average linearly fitted.

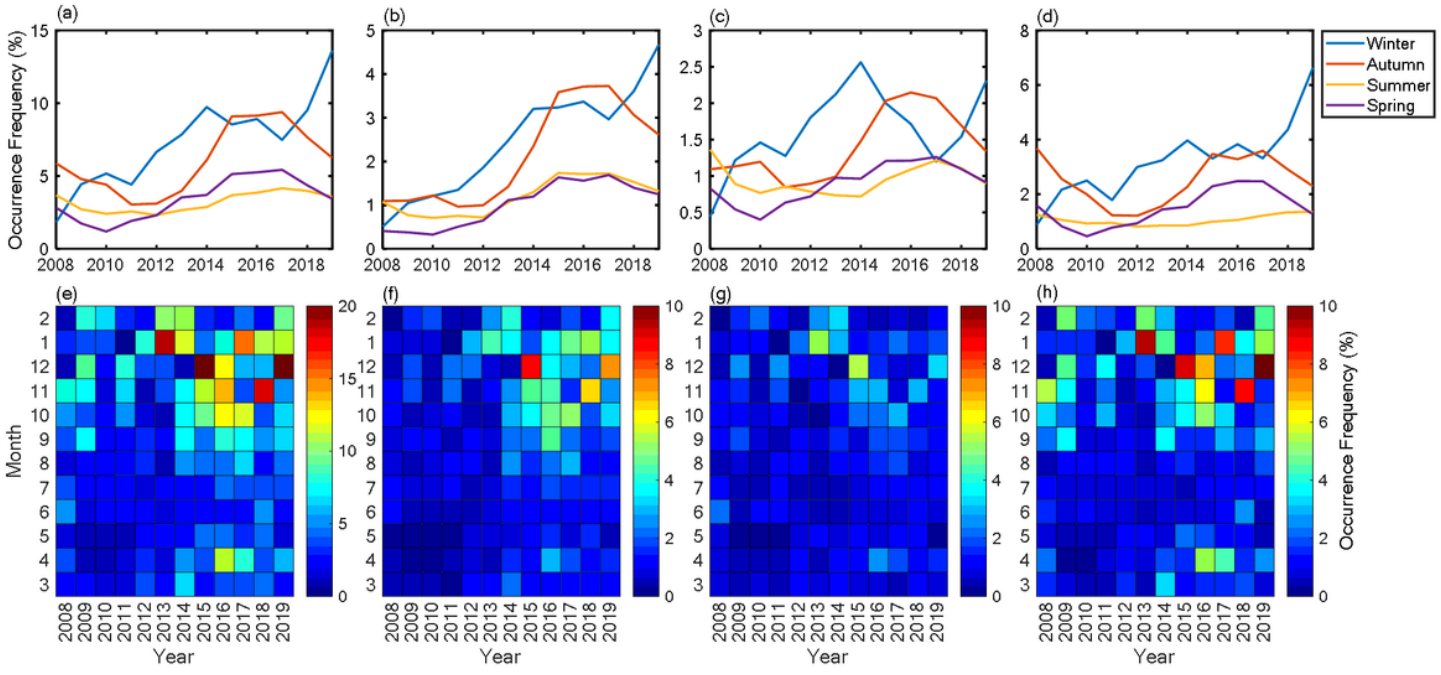

Figure 8

Trends of the 3-year moving average occurrence frequencies of (a) total fog, (b) light fog, (c) dense fog, and (d) extreme fog in spring (MAM), summer (JJA), autumn (SON), and winter (DJF) among the 122 meteorological stations from 2008-2019. Monthly frequencies of (e) total fog, (f) light fog, (g) dense fog, and (h) extreme fog.

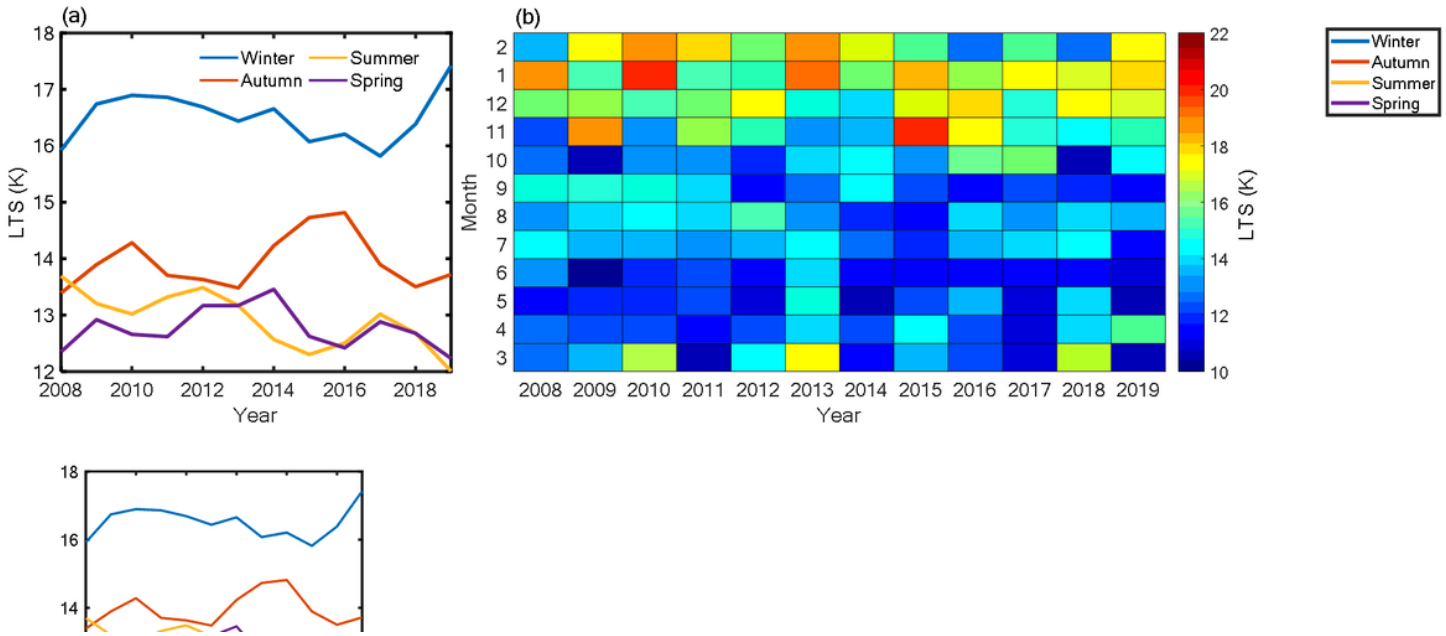

Figure 9

(a) Trends of the spatial average 3-year moving average lower-tropospheric stability (LTS) in spring (MAM), summer (JJA), autumn (SON), and winter (DJF) in Shandong Province from 2008-2019. (b) Monthly spatial average LTS.

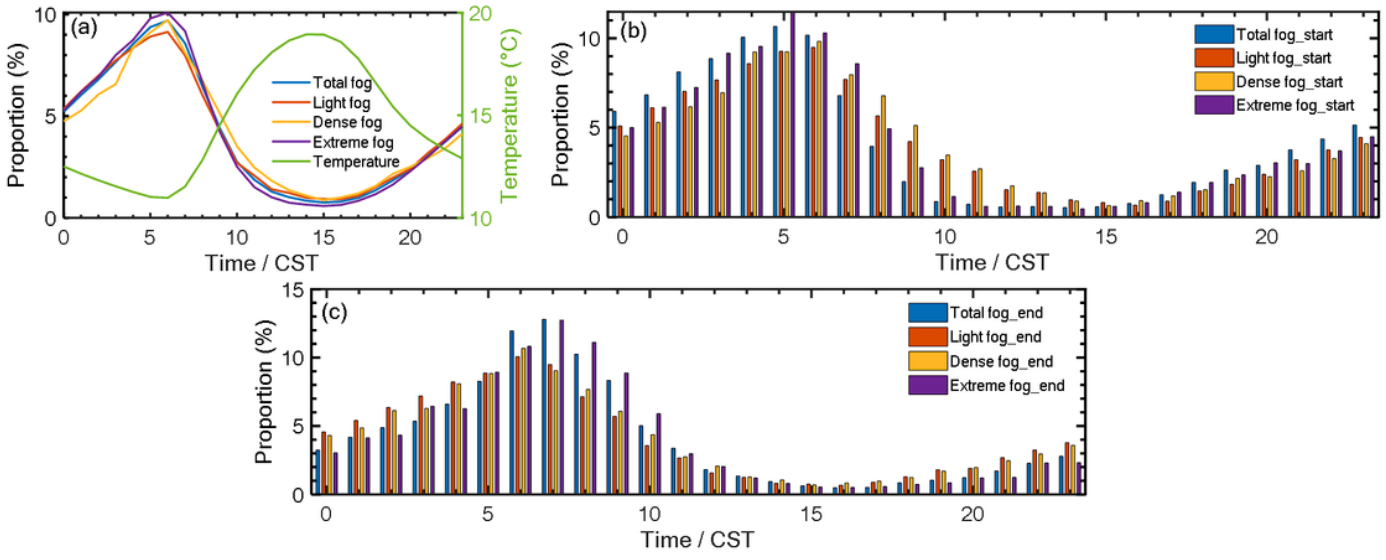

Figure 10

(a) Proportions of total fog (blue line), light fog (red line), dense fog (orange line), and extreme fog (purple line) in each hour and the diurnal variation in temperature (green line) from 2016-2019. (b) Diurnal variation of the fog start time. (c) Same as in (b) but for the end time. CST represents China Standard Time.

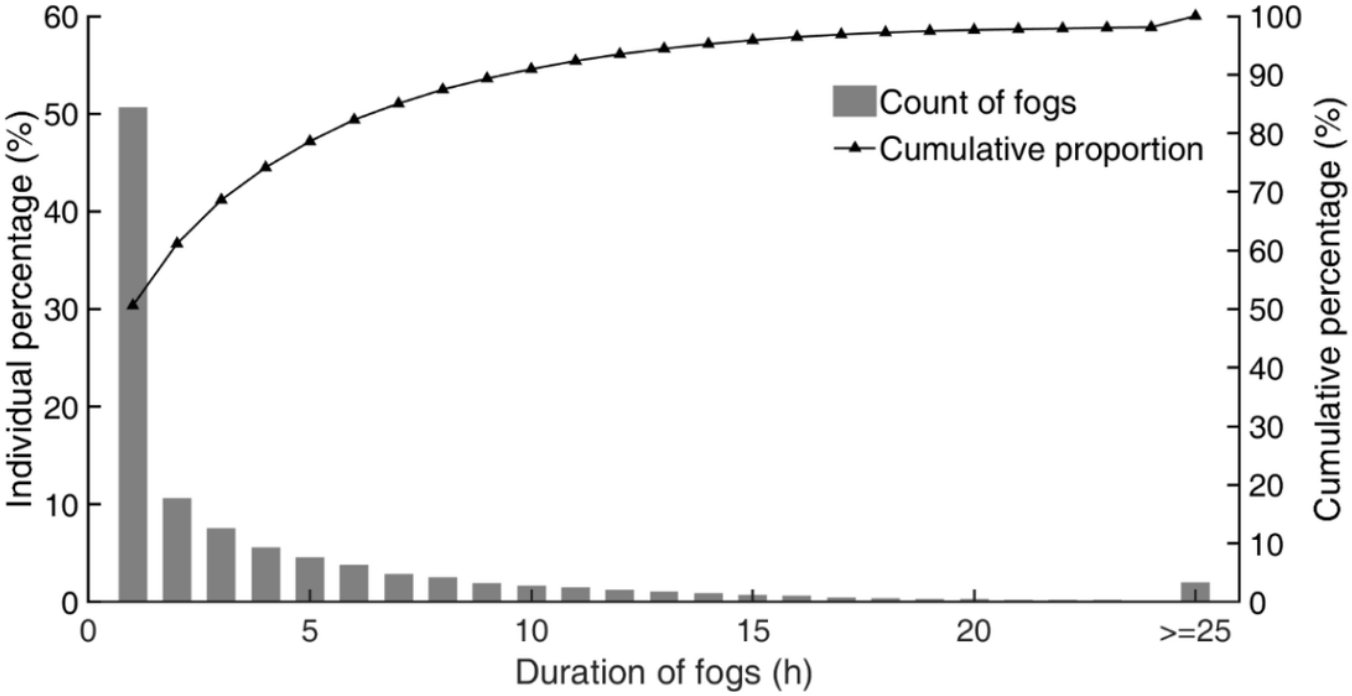

Figure 11

Statistical histogram of the fog duration distribution from 2016-2019. The black polyline is the cumulative percentage (%).